Room-temperature radiation effects in Al-doped Y-bar quartz

1994 J. Phys.: Condens. Matter 6 4457

(http://iopscience.iop.org/0953-8984/6/24/008)

J. Phys.: Condens. Matter 6 (1994) 4457–4464. Printed in the UK

Room-temperature radiation effects in Al-doped Y-bar quartz

Xi-Qi Feng†, Tong B Tang‡ and Wei-Zhuo Zhong†

† Shanghai Institute of Ceramics, Academia Sinica, Shanghai 200050, People's Republic of China

‡ Physics Department, Hong Kong Baptist College, Kowloon Tong, Kowloon, Hong Kong

Received 22 December 1993, in final form 3 March 1994

Abstract. Infrared and optical spectra were measured for synthetic quartz in Y-bar form, as it received progressive dosage of γ-irradiation. The γ-induced coloration varied in intensity over different growth regions of the Y-bar, in proportion to the density of aluminium impurities, the latter being dependent on the growth speed of the region in question as well as the polarization effect of the x-axis. From the variations in absorbance within the conventionally designated S_4, e_2 and A_1 absorption bands, we deduce that, over a broad range of dosage, Al–OH defects increased continuously while as-grown OH sites hardly decreased in concentration. This indicates the presence of another kind of as-grown H centre that does not show up in IR absorption. It is most noticeable in the $-x$ region, which, like air-swept quartz, has a low radiation susceptibility.

1. Introduction

There has been persistent interest over the past two decades in understanding the radiation responses of α-quartz and their relation to its impurities (see, e.g., King and Sander (1975), Martin (1988) and Bahadur (1992)). The interest stems from its widespread use in ultra-stable oscillators for satellite communication and aerospace guidance systems, in which its radiation susceptibility is a critical consideration (see, e.g., Brunet *et al* (1992)). This susceptibility arises from the radiation-induced mobility of point defects associated with impurities, which leads to modification in materials constants and hence to a change in device performance.

The ubiquitous dopant in synthetic quartz is Al^{3+}, which substitutes for isoelectronic Si^{4+} (Weil 1975, 1984). The existence of interstitial Al^{3+} is energetically unfavourable (Iwasaki and Iwasaki 1993). Since quartz is cultured in an environment rich in alkalis, interstitial $M^+ \equiv Li^+$, Na^+ or K^+ ions have a significant presence in as-grown samples, as does H^+, form the growth solution. Protons may also be introduced by the fabrication process of electrodiffusion or 'sweeping' in air or hydrogen (King 1959), during which they replace the M^+ interstitials. Depending on the charge compensator, therefore, four main types of point defect may form (Lipson and Kahan 1985). They are

(1) the Al–M centre,
(2) as-grown OH,
(3) Al–OH sites, and
(4) Al-h,

where the hole is created during sweeping in vacuum or inert gas, or during irradiation by x- or γ-rays or by electrons, when an electron is removed from a non-bonding orbital of

0953-8984/94/244457+08$19.50

an oxygen ion adjacent to the substitutional aluminium impurity ion Al_{Si} (O'Brien 1955, Weaver and Schindler 1964). At room temperature, another effect of the ionizing radiation is to trigger the motion of these defects along the relatively open c-axis channels of quartz, resulting in their redistribution and therefore altered materials properties.

In this work, with the help of photo-spectrometry and infrared spectroscopy, we have examined the relative concentrations of as-grown OH, Al–OH and Al–h as well as their changes with room-temperature radiation dose. The sample studied was grown from a y-axis seed crystal. In this so-called Y bar, which is the type commonly found in piezoelectric applications, individual growth regions contain different impurities and defect densities and thus exhibit different radiation responses. Our study should provide useful information for the non-destructive assessment of quality in quartz and for the improvement of radiation susceptibility.

2. Experimental details

A quartz Y bar was cultured in a solution of NaOH (1 N) and KOH (0.3 N) containing 0.5 wt.% $Al(OH)_3$. Its $z(0001)$ face grows the most rapidly, followed by the s (i.e. the trigonal bipyramid) face and then the $+x(\bar{1}\bar{1}20)$ face, whereas the $-x\{11\bar{2}0\}$ face grows the most slowly. Aluminium concentrations in different growth regions of this stone were determined with a Philip PW-1404 x-ray fluorescence spectrometer, whose x-ray beam diameter was about 4 mm.

The Y bar was then γ-irradiated at room temperature with a Co^{60} source for five successive intervals totalling 1 h, after which the cumulative dose reached 0.2 MGy (1 Gy = 100 rad). Different regions showed various degrees of coloration, and their absorption spectra within the range 300–900 nm were recorded after each interval in a Shimazu UV-265 photospectrometer. Infrared absorption between 3700 and 3100 cm^{-1} was measured with a Nicolet 7000 Fourier spectrometer, with the incident IR beam, 5 mm in diameter, parallel to the y-axis of the sample.

Previous infrared studied on the structures of defects in quartz were mostly conducted at low temperatures, to attain high spectral resolution. However, the aim of the present work is a comparison of the defect concentration in different growth regions or before and after irradiation, but not a determination of their absolute magnitudes. Our measurements have therefore proceeded at ambient tempertature.

Table 1. Densities of Al impurities.

Region	Concentration (normalized)
z	1.0
s	0.98
$+x$	0.94
$-x$	0.90

3. Results

Table 1 lists the relative Al dopant levels determined for different regions in the Y bar. After irradiation, as figure 1 shows, its z growth region turned into a non-uniformly black colour,

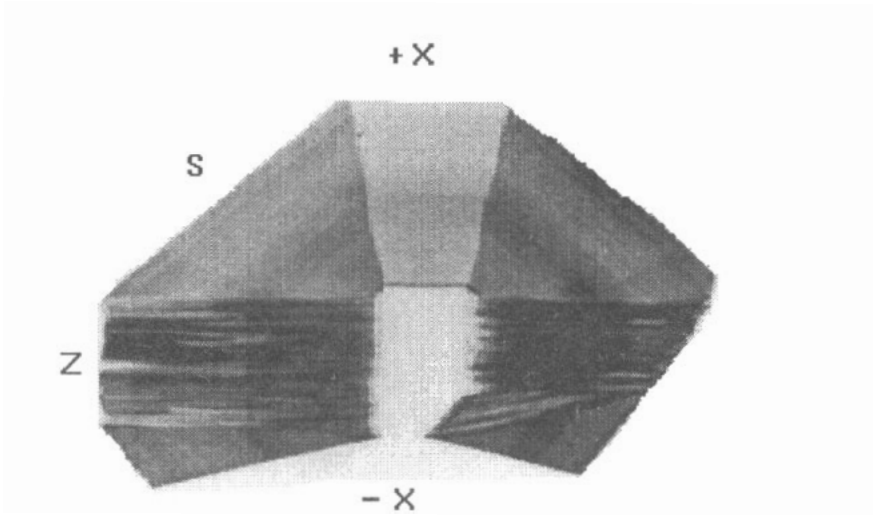

Figure 1. Coloration in different growth regions after the Y bar has received 0.2 MGy cumulatively at room temperature.

but the s region was less dark and the $+x$ least black, while the $-x$ region remained clear even after receiving a total dosage of 0.2 MGy. Coloration thus appeared to be proportional to the Al level. Photospectrometric data (figure 2) confirmed this observation. In the figure, three broad Gaussian absorption bands are labelled A_1–A_3 following Schirmer (1976), whose polarized absorption spectra obtained at 77 and 294 K can resolve the overlapping A_2 and A_3 bands. Schirmer ascribes them to optical transitions of holes on non-bridging oxygen ions adjacent to Al_{Si} sites, from one equivalent O^{2-} site to another, against the self-induced trapping potential. Koumvakalis (1980) has also found support for the origin of the A_1–A_3 bands in Al–h, by establishing the correlation between visible optical absorption and ESR signal from $(Al_e^+)^0$ centres under various irradiation conditions.

We now consider the infrared measurements. It has been demonstrated that, in as-grown synthetic quartz, there are only four significant bands of non-intrinsic origin, with peaks at 3348 (or 3353), 3396 (or 3400), 3437(8) and 3581 cm^{-1} (Kats 1962, Brown and Kahan 1975, Bahadur 1989). These near-infrared features, designated S_1–S_4, are easily resolved at 80 K but, at room temperature, only S_4 at 3581 cm^{-1} remains relatively narrow whereas the rest are greatly broadened. Figure 3 shows the room-temperature spectra measured of the s and the $-x$ regions in our sample; those for the z and the $+x$ regions resemble that of the s region and have thus been omitted. In each of these spectra a broad absorption maximum extends from 3700 to 3100 cm^{-1} and relates possibly to lattice vibration. Superimposed on this background stand two sharp peaks, at 3582 cm^{-1} (i.e. S_4) and at 3606 cm^{-1}, for the case of the s region. In the $-x$ spectrum, the background is more intense; only S_4 remains distinguishable but the feature at 3606 cm^{-1} is absent. After receiving 0.2 MGy, the s region lost both peaks completely while S_4, for $-x$, decreased in intensity. On the other hand, in all spectra, new bands were formed at 3306, 3366 and 3424 cm^{-1}. The first two are the $e_{1,2}$ bands that have been reported for irradiated or air-swept synthetic quartz and attributed to Al–OH centres (Kats 1962, Halliburton *et al* 1981, Lipson and Kahan 1985).

We monitored the heights of the S_4, the e_2 and the A_1 bands as measures of the respective densities of as-grown OH, Al–OH and Al–h. Since only changes in these concentrations are of interest, it suffices to compare relative peak heights rather than integrated band areas.

The series of peak heights as a function of accumulated radiation dose, in the case of the

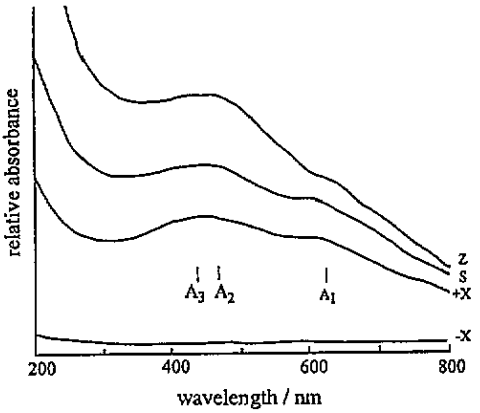

Figure 2. Visible-light absorption spectra for the sample photographed in figure 1.

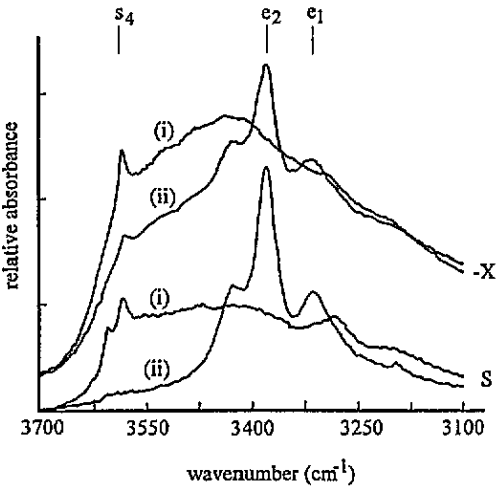

Figure 3. Room-temperature IR spectra of the s and $-x$ regions before irradiation (curve (i)) and after irradiation (curve (ii)).

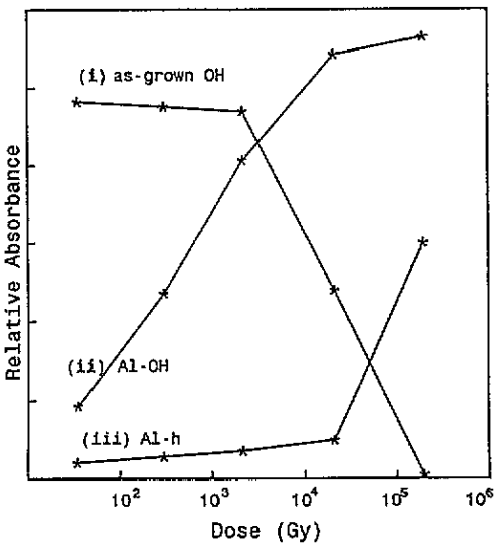

Figure 4. Variations in absorbance with irradiation dosage, for the s region, of the S_4 (curve (i)), e_2 (curve (ii)) and A_1 (curve (iii)) bands, which indicate the changes in concentrations of as-grown OH (curve (i)), Al–OH (curve (ii)) and Al–h (curve (iii)), respectively.

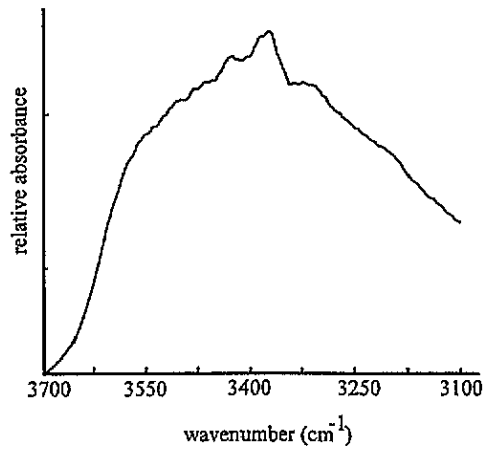

Figure 5. Room-temperature IR spectrum of the $-x$ region after receiving 0.2 MGy, showing the disappearance of the S_4 band and a much reduced e_2 band.

s region, are depicted in figure 4. On the basis of the aforesaid reasoning, we deduce that the concentration of Al–OH increased continuously with increasing dosage, but a significant amount of OH growth defects did not disappear until well after the dose reached 2 kGy, demonstrating that their radiation-induced dissociation did not constitute the sole source of Al–OH production. This is further corroborated by the deduction that, at an excess of

2 kGy, as-grown OH defects did start to dissociate but the production curve for Al–OH hardly changed its slope. Indeed, it saturated when the dosage exceeded 20 kGy, probably as a consequence of Al^{3+} depletion. Above that same dosage, in contrast, Al–h rose rapidly in concentration from an initially low level. This observation is in agreement with the proposition of Lipson and Kahan (1984), that Al–h defects form only after as-grown OH defects have nearly completely disappeared.

A similar observation was made for the $-x$ region, which quickly turned black once its S_4 band disappeared, except that the critical dosage was much greater, but varied considerably from sample to sample. Figure 5 shows its absorption in the near-infrared range.

4. Discussion

4.1. Distribution of Al^{3+} defects

Al impurities play a key role in the formation of colour centres in quartz. Generally speaking, the higher its concentration, the darker will be the visible coloration due to irradiation, and which therefore may serve as a means for 'visualizing' the distribution of Al^{3+} defects. These are found mainly in two types of place, i.e. growth faces that result from temperature fluctuations during crystal growth, and the flutes formed by trigonal pyramids on the $z(0001)$ face; hence there is non-uniform coloration in this region. Point defects develop most easily when growth occurs most rapidly, where consequently Al is most concentrated. Another factor influencing the distribution in Y-bar quartz is its axis polarity. The growth unit for quartz is, according to Zhong (1979), the tetrahedral structure consisting of a silicon atom surrounded by four Si–O planes, and the three free poles of each of these four Si are hydrated (figure 6). The surface of this growth unit, $Si_5O_4(OH)_{12}$, is therefore negatively charged so that, during crystal growth, the $+x$ region repels Al^{3+} whilst the $-x$ region attracts Al^{3+}.

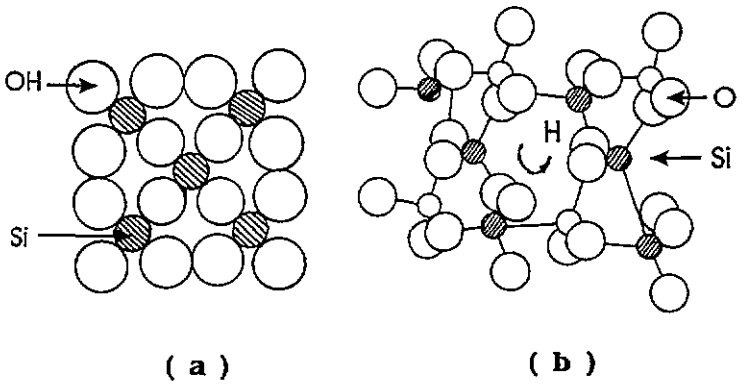

Figure 6. Growth model for quartz: (a) surface hydration of the growth unit; (b) helical channel along the *c* axis, formed by conjugate pairs of growth units.

4.2. IR-inactive hydrogen centre and radiation-insensitive as-grown OH

As-grown OH constitutes the well known non-Al-associated hydrogen defect in synthetic quartz. Its detailed configuration remains as yet unclear, but the most commonly accepted model involves a water molecule incorporated during crystal growth, breaking the Si–O–Si bond to end up as two non-bridging Si–OH centres (Brunner *et al* 1961). Together with Al–M, as-grown OH dissociates under the action of ionizing radiation and, at room temperature, the alkali metal M diffuses to a certain acceptor site, leaving Al–OH behind. It should then follow that, as the dosage increases, as-grown OH will drop in concentration, but that of Al–OH will continue to rise until as grown OH or Al^{3+} is exhausted. However, as deduced from figure 4, until the *s* region received a fairly large dose, little change in the as-grown OH accompanied the continuous increase in Al–OH. This indicates an additional H^+ source, not associated with Al^{3+}, that dissociates under irradiation more readily than as-grown OH, but which does not contribute to IR spectra.

A candidate for the precursor of such non-Al-associated but IR-inactive hydrogen is Na–OH (Lipson and Kahan 1985). During crystal growth, the mineralizer used is usually NaOH or $NaCO_3$, which in solution also forms NaOH, and NaOH may enter the host lattice, giving rise to hydrogen-containing defects. Indeed, according to the model proposed by Zhong (1979) for the growth unit in quartz, the five-chain-molecular $Si_5O_4(OH)_{12}$ has, as explained above (figure 6), a negatively charged surface, resulting in its easy incorporation on the positive $+x$ face, whereby more amorphous gelatinous molecules are available there than on the $-x$ face. Thus, the impurity anions will be scarce there, but instead they aggregate on the $+x$ face, as has been found experimentally (Brown and Thoms 1960). In this work the samples investigated were grown with NaOH and KOH as the mineralizers, and the abundance of Na^+ and K^+ on the $-x$ face may account for its low radiation sensitivity.

Instead of IR-inactive OH dipoles, there may be other kinds of H-containing species such as Si–H (if of small dipole moment) and atomic or molecular dissolved hydrogen (Hartwig and Vitko 1978, Stone *et al* 1984, Graebner *et al* 1985). Indeed, Robinson (1985) has given a comprehensive discussion on H 'reservoirs' not detectable by IR or by ESR. An alternative explanation for the radiation insensitivity of the $-x$ region is therefore its abundance of such H centres, which later contribute to the as-grown OH band.

4.3. Radiation effects

Al–h is perhaps the best-characterized point defect in quartz. It is responsible for the visible absorption bands A_1 and A_2 (Schirmer 1976, Koumvakalis 1980), and the ensuing coloration degrades crystal quality. Nevertheless, its formation depends much on impurities and treatment (such as sweeping) and varies in degree over different regions of even the same specimen. In this work on a Y bar, the $-x$ region did not blacken after receiving a relatively large dose, implying radiation insensitivity. A probable explanation has been offered above.

Like room-temperature irradiation, sweeping in vacuum or in an inert atmosphere also produces Al–h. The sequence of defect formation (Lipson and Kahan 1984) is as follows.

(1) Al–M centres dissociate, as-grown OH defects are reduced and Al–OH centres form as an intermediate state.

(2) As-grown OH defects are depleted and Al–OH centres dissociate. Thus

(3) Al–h are produced.

In principle, a similar chain of events should occur in the case of irradiation (Lipson and Kahan 1985).

Two situations may then arise in accordance with an initial condition, namely the level of as-grown OH defects including IR-inactive hydrogen centres. If initially their concentration is low, they will be depleted before Al–M, and in their absence the leftover Al–M dissociates to form Al–h directly. This should be the situation applicable to the blackened s region discussed in our work. Alternatively, if originally there are many as-grown OH, some will remain after all Al–M centres have gone, few Al–h defects are produced and the crystal therefore stays clear. Such is the case for the irradiated $-x$ region. Indeed, it bears close similarity to the situation in air-swept crystals, in having Al–M depleted, and most defect sites saturated and passivated with hydrogen, to exist as Al–OH (or as-grown OH). The only difference relates to alkali metal ions, present in the $-x$ region, but which have electrodiffused out from swept samples. Nevertheless, both kinds of quartz excel in terms of radiation response, since in neither can ionic exchange take place.

5. Conclusions

(1) Room-temperature irradiation causes coloration in Al-containing quartz. By this means, the relative Al concentrations and defect distributions may be visualized in different growth regions (except for $-x$) of a Y bar. The levels of Al in these regions (z, s, $+x$ and $-x$) are determined by the crystal growth speed and axis polarization.

(2) Room-temperature IR and visible spectroscopies may serve to monitor the densities of as-grown OH, Al–OH and Al–h defects in various regions. As irradiation proceeds, the concentration of Al–OH increases but that of as-grown OH remains quite unchanged. This points to the existence of IR-inactive hydrogen centres. It is most noticeable in the $-x$ region where Na^+ and some K^+ impurity ions aggregate.

(3) The $-x$ region has high concentrations of as-grown OH and IR-inactive hydrogen defects, an abundance of Na–OH but a relatively low density of Al–Na—hence its radiation insensitivity, like air-swept quartz. Of course, for the same reason, namely high defect densities, if used as an oscillator crystal it has a high resistance and low Q factor, but this may be tolerated in applications where radiation hardening is the prime consideration.

Acknowledgments

This work was sponsored by the National Science Foundation of China and supported by a Faculty Research Grant from the Hong Kong Baptist College. The FTIR spectrometer is a Chemistry–Physics Joint Facility in the latter institution. We would like to thank the referee for his/her constructive criticism.

References

Bahadur H 1989 *J. Appl. Phys.* **66** 4973

—— 1992 *IEEE Trans. Nucl. Sci.* **39** 2170

Brown C S and Thoms L A 1960 *J. Phys. Chem. Solids* **13** 467

Brown R N and Kahan A 1975 *J. Phys. Chem. Solids* **36** 467

Brunet M, Dutrey J F, Laporte J B, Bourriau J and Calvel P 1992 *Proc. 6th Eur. Frequency Time Forum* (Noordwijk: European Space Agency) p 431

Brunner G O, Wondratschek H and Laves F 1961 *Z. Electrochem.* **65** 735
Graebner J E, Lemaire P J, Allen L C and Haemmerle W H 1985 *Appl. Phys. Lett.* **46** 839
Halliburton L E, Koumvakalis N, Markes M E and Martin J J 1981 *J. Appl. Phys.* **52** 3565
Hartwig C M and Vitko J 1978 *Phys. Rev.* B **18** 3006
Iwasaki F and Iwasaki H 1993 *Japan. J. Appl. Phys.* **32** 893
Kats A 1962 *Philips Res. Rep.* **17** 133
King J C 1959 *Bell Syst. Tech. J.* **38** 573
King J C and Sander H H 1975 *Radiat. Eff.* **26** 203
Koumvakalis N 1980 *J. Appl. Phys.* **51** 5528
Lipson H G and Kahan A 1984 *IEEE Trans. Nucl. Sci.* **31** 1223
—— 1985 *J. Appl. Phys.* **58** 963
Martin J J 1988 *IEEE Trans. Ultrason. Ferroelec. Freq. Control* **35** 288
O'Brien M C M 1955 *Proc. R. Soc.* A **231** 404
Robinson P 1985 *PhD Thesis* University of Oxford
Schirmer O F 1976 *Solid State Commun.* **18** 1349
Stone J, Chraplyvy A R, Wiesenfeld J M and Burrus C A 1984 *Bell Lab. Tech. J.* **63** 991
Weaver H E and Schindler P 1964 *Naturwissenschaften* **51** 81
Weil J A 1975 *Radiat. Eff.* **26** 261
—— 1984 *Phys. Chem. Minerals* **10** 149
Zhong W Z 1979 *Acta Phys. Sinica* **28** 240